Science of the Total Environment 616–617 (2018) 1181–1189

Contents lists available at ScienceDirect

Science of the Total Environment

journal homepage: www.elsevier.com/locate/scitotenv

# Carbon biogeochemical cycle is enhanced by damming in a karst river

Qiong Han [a], Baoli Wang [a,*], Cong-Qiang Liu [b], Fushun Wang [c,*], Xi Peng [b], Xiao-Long Liu [d]

[a] Institute of Surface-Earth System Sciences, Tianjin University, Tianjin 300072, China
[b] State Key Laboratory of Environmental Geochemistry, Institute of Geochemistry, Chinese Academy of Sciences, Guiyang 550002, China
[c] Institute of Applied Radiation, School of Environmental and Chemical Engineering, Shanghai University, Shanghai 201800, China
[d] Tianjin Key Laboratory of Water Resources and Environment, Tianjin Normal University, Tianjin 300387, China

## HIGHLIGHTS

- After damming, carbon species developed obvious stratification in water profile.
- Carbon species showed larger variations in reservoir than in corresponding river.
- After damming, biological activity became key factor and accelerated carbon cycle.

## GRAPHICAL ABSTRACT

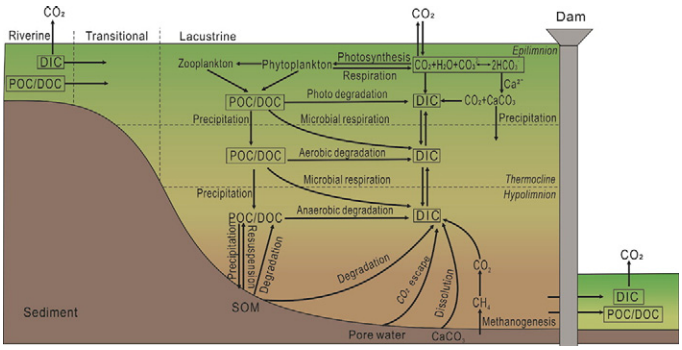


## ARTICLE INFO

*Article history:*
Received 7 June 2017
Received in revised form 11 September 2017
Accepted 20 October 2017
Available online 27 October 2017

Editor: G. Ashantha Goonetilleke

*Keywords:*
Stable carbon isotope
Carbon cycle
Phytoplankton
Dam construction
Wujiang River

## ABSTRACT

Currently, there is a lack of systematic knowledge concerning carbon (C) biogeochemical cycles in impounded rivers. In this study, we investigated different C species and related environmental factors from July 2007 to June 2008 and from May 2011 to May 2012 in the impounded Wujiang River, SW China to understand the influence of dam construction on the riverine C cycle. The results showed that average concentrations of dissolved $CO_2$, dissolved inorganic C (DIC), dissolved organic C, and particulate organic C (POC) were 81.73 μmol/L, 2283.55 μmol/L, 158.11 μmol/L, and 37.54 μmol/L, respectively. Meanwhile, $\delta^{13}C_{DIC}$ ranged from −10.07‰ to −4.92‰ with an average of −8.33‰, while $\delta^{13}C_{POC}$ ranged from −35.30‰ to −22.28‰ with an average of −29.20‰. Thermal and chemical stratifications developed seasonally and exerted a significant influence on the C cycle of the released water. The C species and related $\delta^{13}C$ showed remarkable heterogeneity in time and space. Evidence from $\delta^{13}C$ demonstrated that the C system in this river was primarily influenced by carbonate weathering, whereas in the reservoir, it was primarily controlled by algal activity. The coefficients of variance for different C species in the reservoir and released water were higher than those in the river. Our study indicated that biological activity became a key controlling factor for the C biogeochemical cycle and accelerated it after damming, especially in the warm seasons. The results of this study have important implications for understanding the C cycle in elongated and deep reservoirs.



* Corresponding authors at: 92 Weijin Road, Tianjin 300072, China.
*E-mail addresses:* hanqiong2015@tju.edu.cn (Q. Han), baoli.wang@tju.edu.cn (B. Wang), liucongqiang@vip.skleg.cn (C.-Q. Liu), fswang@shu.edu.cn (F. Wang), pengxi@vip.skleg.cn (X. Peng), liuxiaolong@mail.tjnu.edu.cn (X.-L. Liu).

https://doi.org/10.1016/j.scitotenv.2017.10.202
0048-9697/

## 1. Introduction

Dam construction has become one of the most disturbing anthropogenic activities on natural rivers. Approximately 70% of the world's rivers were intercepted by dams (Kummu and Varis, 2007) with 58,266 dams with heights over 15 m, among which 23,842 were in China by the year of 2015 (http://www.icold-cigb.org/). Almost all rivers in China were intercepted at various levels and became impounded rivers. After cascading hydropower exploitation, the successional and gradually varied water line of a natural river turns to a stepped one. With river impoundment, the flow rate becomes slower, and the residence time increases. Meanwhile, under artificial regulation of reservoir water, the magnitudes of flood peaks are reduced, the downstream flow regime is altered, and the total runoff volume is affected, resulting in further changes to the hydrological conditions in the river, floodplain and even coastal delta (Mccartney et al., 2001). Therefore, large-scale damming interrupts the river continuum and destroys the 'flood pulse' pattern. Damming also changes the matter and energy fluxes in the original river ecosystem and thereafter directly affects the biogeochemical behaviour of nutrient elements, such as carbon (C), phosphorus, and silicon (Humborg et al., 2000; Zhou et al., 2013; Peng et al., 2014). The changes caused by dams ultimately influence species composition, habitat heterogeneity, and relevant ecological functions (Karr, 1991).

The fluxes of C in impounded rivers are an important part of the terrestrial C budget (Aufdenkampe et al., 2011; Regnier et al., 2013). As such, fully understanding the processes and mechanisms of the C biogeochemical cycle is crucial for accurately estimating the C budget in impounded rivers. However, there is still a lack of relevant knowledge. For example, the choice of existing patterns, the age pattern or latitudinal pattern, for estimating global reservoir $CO_2$ emissions (Barros et al., 2011) is still open to discussion, primarily because the effects of retention time on $CO_2$ flux are generally not taken into account (Wang et al., 2015).

The water chemistry of karst rivers is primarily affected by the weathering of carbonate rocks (e.g., Chetelat et al., 2008), which can consume atmospheric $CO_2$. Therefore, the karst river system can be considered a carbon sink (Sironić et al., 2016; Zeng et al., 2016), and it may act as a buffer against elevated atmospheric $CO_2$ concentrations (Liu and Dreybrodt, 2015). However, Cole et al. (2007) reported that streams and rivers are the net input source of $CO_2$ to the atmosphere. Khadka et al. (2014) suggested that soil respiration and carbonate dissolution are the primary controls on C fluxes in karst rivers. Nevertheless, it is still unclear whether this phenomenon is observed in karst river-reservoir systems. River erosion on karst landscapes generally results in the formation of deep canyons, and deep and elongated reservoirs are prone to form after dam interception. These reservoirs not only have limnological characteristics, such as water stratification, but also features of artificial regulation, such as discharge of bottom water and counter-seasonal impounding (Liu et al., 2009; Wang et al., 2010). In addition, cascading hydropower exploitation leads to more complex cumulative effects. Given these features, the karst river-reservoir system forms a unique C biogeochemical cycle.

In this study, we investigated the C system and related environmental factors in the impounded Wujiang River, SW China. The purpose of this study was to understand the C biogeochemical cycle and to discern the controlling factors in the karst river-reservoir system. This study provides additional insights into the influence of dam construction on the C biogeochemical cycle, as well as the theoretical basis for accurately estimating the C budget in impounded rivers of karst systems.

## 2. Materials and methods

### 2.1. Study area

The Wujiang River is the largest tributary on the south bank of the upper reaches of the Changjiang (Yangtze) River and the largest river in Guizhou Province, located in SW China. With a total length of 1037 km and a drainage area of 88,267 $km^2$, the Wujiang River is one of the most developed rivers for hydropower exploitation. This river has many reservoirs with different histories and different trophic levels. Carbonate rocks are widespread in the Wujiang Basin, and the predominant lithological characteristics of the upper reaches are basalt, Triassic carbonate rock, and coal-bearing petrofabric (Wang et al., 2004). The region has a subtropical monsoonal humid climate with an average annual temperature of 12.3 °C. Precipitation occurs from May to October, accounting for 75% of the total annual precipitation. In this study, the Wujiangdu Reservoir (Table 1), located in the upper reaches of the Wujiang River, was investigated, and the inflow, reservoir, and released waters (W1–W3) were sampled (Fig. 1).

### 2.2. Sampling and analysis

Two field campaigns were conducted, one from 2007 to 2008 and another from 2011 to 2012. From July 2007 to June 2008 (2007–2008), the surface water (upper 0.5 m) was sampled monthly. According to thermal stratification, site W2 was also sampled at different depths (i.e., 5 m, 15 m, 30 m, and 60 m) in July, October, January, and April, representing summer, autumn, winter, and spring, respectively. From May 2011 to May 2012 (2011 − 2012), only the surface water was sampled twice per month. The pH, water temperature (T), and dissolved oxygen (DO) were measured in situ with an automated multiparameter profiler (model YSI 6600) that was calibrated on site, and alkalinity (ALK) was determined by titration with HCl in the field. The concentration of chlorophyll (Chl) was measured with a YSI 6600 during the 2007–2008 survey and with a Phyto-PAM (WALZ, Germany) during the 2011–2012 survey. Water samples were filtered through glass fibre filters (0.70 μm, Whatman GF/F) immediately after sampling. The filtered water was divided for the analysis of anions, cations, dissolved organic C (DOC), and the C isotope composition of dissolved inorganic C ($\delta^{13}C_{DIC}$). A saturated $HgCl_2$ solution was added to the vials containing the filtered water for $\delta^{13}C_{DIC}$, and the vials were immediately sealed with parafilm without any void space. The particulate matter left on the filters was used for analysing the concentration and C isotope composition of particulate organic C ($\delta^{13}C_{POC}$). For the 2007–2008 survey, $\delta^{13}C_{POC}$ was only determined in July, October, January, and April.

Anions ($SO_4^{2-}$, $Cl^-$, and $NO_3^-$) were analysed using high-performance liquid chromatography ICS-90 (Dionex, USA), and major cations ($Ca^{2+}$, $Mg^{2+}$, $K^+$, and $Na^+$) were analysed using inductively coupled plasma-optical emission spectrometry (ICP-OES). These major ions were used to determine ionic strength. $HCO_3^-$, $CO_3^{2-}$, and dissolved $CO_2$ were calculated using ALK, pH, T, and ionic strength according to Maberly (1996) and Peng et al. (2014). POC concentrations were measured using an elemental analyser (Vario macro cube, Germany) and were only measured during the 2011–2012 survey. DOC concentrations were measured using an Aurora 1030 TOC analyser (OI Analytical, USA) and were only measured in the 2007–2008 survey. The $\delta^{13}C_{DIC}$ samples were injected into closed evacuated glass vessels containing concentrated phosphoric acid and then heated at 50 °C to extract $CO_2$ (Atekwana and Krishnamurthy, 1998). The particulate matter on the filters was acidified with dilute hydrochloric acid and oven-dried overnight at 60 °C for measuring $\delta^{13}C_{POC}$. POC was converted to $CO_2$ using the high-temperature (850 °C for 5 h) sealed-quartz combustion method with

**Table 1**
Main characteristics of the Wujiangdu Reservoir.

| | |
|---|---|
| Running age (until 2017) (years) | 39 |
| Drainage area ($km^2$) | 27,790 |
| Average annual discharge ($m^3/s$) | 502 |
| Total storage capacity ($10^8$ $m^3$) | 23 |
| Height of dam (m) | 165 |
| Hydrological retention time (days) | 53 |
| Normal water level (m) | 790 |

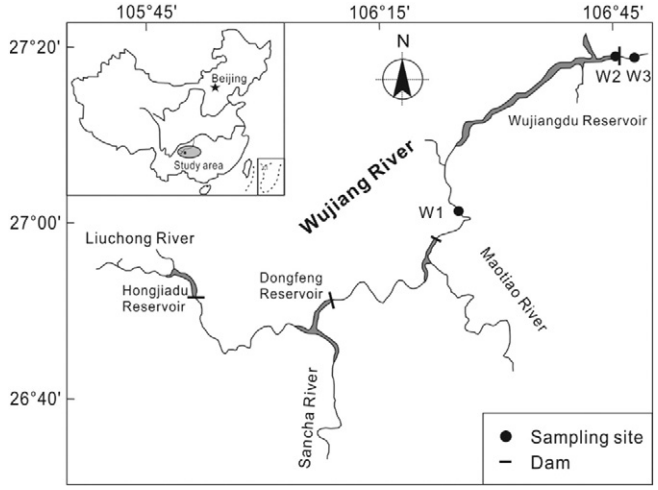


**Fig. 1.** Map showing study area and sampling sites.

copper oxide as the oxidant (Buchanan and Corcoran, 1959). The extracted $CO_2$ was analysed on a MAT252 mass spectrometer. The $\delta^{13}C$ measurements were normalised to the Pee Dee Belemnite standard (PDB) with an analytical precision of ±0.1‰: $\delta^{13}C$ (‰) = [($R_{sample}$ − $R_{PDB}$) / $R_{PDB}$] × 1000.

Statistical analysis of the data was conducted with the software SPSS (version 22.0; IBM SPSS). A Pearson's correlation coefficient analysis was conducted.

## 3. Results

### 3.1. Basic physical, chemical and biological parameters

The average concentrations of T, pH, DO, and Chl were 17.53 °C, 7.91, 8.44 mg/L, and 6.26 μg/L, respectively. The measured parameter values in the two surveys are listed in Table 2. The T of the inflow, reservoir, and released waters showed a similar trend, with T increasing from January and reaching a maximum in July. This finding was consistent with our previous study (Wang et al., 2013). The pH and DO of the reservoir showed a temporal pattern similar to the one for the T of the reservoir. In the inflow and released waters, the temporal variations in pH in 2007–2008 were different from those in 2011–2012, but DO variations were similar, with higher DO concentrations in the cold seasons than in the warm seasons. The Chl concentrations also had similar variations in 2007–2008 and in 2011–2012, with higher Chl concentrations in the warm seasons than in the cold seasons.

Thermal stratification in the water column developed seasonally in the Wujiangdu Reservoir (Fig. 2). T, pH, and DO became stratified in April, and the stratification tended to disappear in October. The thermocline was between the depths of 8 m and 23 m. T, pH, and DO displayed large variation in the epilimnion and less variation in the hypolimnion. Generally, Chl concentration decreased with increasing water depth. During the stratification period, the variation was more obvious, and the amplitude of variation in July reached 81 μg/L (Fig. 2d).

### 3.2. Dissolved $CO_2$ ($CO_2$(aq))

Average concentrations of $CO_2$(aq) were 68.86 μmol/L in the inflow water, 52.45 μmol/L in the reservoir, and 123.88 μmol/L in the released water. There was little temporal variation in the $CO_2$(aq) concentration of the inflow water, but larger fluctuations existed in the reservoir and released water, with amplitudes of approximately 130 μmol/L and 350 μmol/L, respectively (Fig. 3a, b). In the reservoir, $CO_2$(aq) concentrations showed a clear seasonal pattern and were lower in the warm seasons than in the cold seasons. Mean $CO_2$ concentrations for 2011–2012 compared to 2007–2008 were lower in the river and released waters and greater in the reservoir. As a whole, the released water had a distinctly higher $CO_2$(aq) concentration than the other water bodies (Table 2).

In the water column, the $CO_2$(aq) concentration of the surface water was highest in autumn, with a value of 127.57 μmol/L, and lowest in summer, with a value of 2.03 μmol/L. The stratification structure started to emerge in spring. In summer, the $CO_2$(aq) concentration was drastically stratified such that the difference between the surface and bottom waters reached a maximum of 163.98 μmol/L. The stratification gradually disappeared in autumn, and the water was fully mixed in winter, with a stable $CO_2$(aq) concentration structure of approximately 52 μmol/L (Fig. 4a).

### 3.3. DIC

Average DIC concentrations were 2262.58 μmol/L in the inflow water, 2240.09 μmol/L in the reservoir, and 2347.99 μmol/L in the released water. The variations in the inflow water, reservoir, and released water differed

**Table 2**
Means and ranges of major biogeochemical variables in the studied areas.

| Term | | 2007–2008 | | | 2011–2012 | | |
|---|---|---|---|---|---|---|---|
| | | W1 | W2 | W3 | W1 | W2 | W3 |
| T (°C) | Max | 21.34 | 28.63 | 20.80 | 24.37 | 29.66 | 24.62 |
| | Min | 10.41 | 10.74 | 10.32 | 9.70 | 9.70 | 9.84 |
| | Mean | 16.31 | 19.66 | 16.27 | 16.81 | 19.75 | 16.40 |
| | SD | 3.76 | 5.86 | 3.73 | 4.14 | 5.97 | 4.76 |
| | CV (%) | 23.06 | 29.79 | 22.9 | 24.63 | 30.22 | 29.02 |
| pH | Max | 8.25 | 9.29 | 7.97 | 8.15 | 8.54 | 8.01 |
| | Min | 7.63 | 7.61 | 7.12 | 7.69 | 7.53 | 7.36 |
| | Mean | 7.86 | 8.38 | 7.65 | 7.93 | 7.95 | 7.70 |
| | SD | 0.18 | 0.54 | 0.23 | 0.11 | 0.30 | 0.18 |
| | CV (%) | 2.31 | 6.46 | 3.02 | 1.44 | 3.77 | 2.40 |
| DO ($mg \cdot L^{-1}$) | Max | 10.58 | 15.43 | 11.63 | 10.68 | 12.38 | 10.19 |
| | Min | 7.43 | 5.14 | 1.12 | 7.80 | 3.76 | 3.15 |
| | Mean | 8.96 | 10.80 | 7.11 | 9.14 | 7.38 | 7.27 |
| | SD | 0.99 | 3.36 | 3.16 | 0.72 | 2.56 | 2.09 |
| | CV (%) | 11.02 | 31.13 | 44.40 | 7.88 | 34.69 | 28.75 |
| Chl ($\mu g \cdot L^{-1}$) | Max | 2.90 | 81.40 | 9.30 | 3.51 | 40.64 | 4.94 |
| | Min | 0.10 | 0.10 | 0.10 | 0.92 | 1.35 | 1.11 |
| | Mean | 0.98 | 18.98 | 2.03 | 2.23 | 11.31 | 2.01 |
| | SD | 1.00 | 22.92 | 3.08 | 1.28 | 10.11 | 0.90 |
| | CV (%) | 101.92 | 120.79 | 151.65 | 57.40 | 89.40 | 44.78 |
| $CO_2$(aq) ($\mu mol \cdot L^{-1}$) | Max | 114.44 | 127.57 | 402.15 | 98.47 | 133.79 | 207.68 |
| | Min | 34.05 | 2.03 | 62.98 | 38.28 | 10.18 | 51.81 |
| | Mean | 77.72 | 42.41 | 141.22 | 60.01 | 62.48 | 106.54 |
| | SD | 23.69 | 45.96 | 91.11 | 16.64 | 37.93 | 43.58 |
| | CV (%) | 30.48 | 108.37 | 64.52 | 27.68 | 61.71 | 40.90 |
| DIC ($\mu mol \cdot L^{-1}$) | Max | 2532.99 | 2598.45 | 3095.77 | 2911.19 | 2551.68 | 2922.13 |
| | Min | 1999.01 | 2123.26 | 2217.29 | 1709.22 | 1623.94 | 1770.68 |
| | Mean | 2335.75 | 2391.01 | 2502.88 | 2189.41 | 2089.16 | 2193.10 |
| | SD | 163.45 | 151.82 | 222.91 | 340.92 | 223.29 | 269.75 |
| | CV (%) | 7.00 | 6.35 | 8.91 | 15.57 | 10.69 | 12.30 |
| POC ($\mu mol \cdot L^{-1}$) | Max | - | - | - | 61.69 | 153.61 | 45.50 |
| | Min | - | - | - | 10.58 | 27.58 | 9.99 |
| | Mean | - | - | - | 26.04 | 62.32 | 24.25 |
| | SD | - | - | - | 11.52 | 34.31 | 11.51 |
| | CV (%) | - | - | - | 44.24 | 55.05 | 47.46 |
| DOC ($\mu mol \cdot L^{-1}$) | Max | 236.42 | 389.92 | 266.33 | - | - | - |
| | Min | 56.33 | 75.67 | 61.08 | - | - | - |
| | Mean | 128.24 | 207.99 | 138.09 | - | - | - |
| | SD | 50.93 | 98.95 | 49.92 | - | - | - |
| | CV (%) | 39.71 | 47.57 | 36.15 | - | - | - |
| $\delta^{13}C_{DIC}$ (‰) | Max | −7.71 | −5.18 | −7.94 | −7.14 | −4.92 | −8.27 |
| | Min | −9.47 | −9.99 | −10.07 | −9.18 | −9.49 | −9.94 |
| | Mean | −8.71 | −7.63 | −9.05 | −8.24 | −7.45 | −8.88 |
| | SD | 0.48 | 1.42 | 0.66 | 0.57 | 1.34 | 0.44 |
| | CV (%) | 5.51 | 18.61 | 7.29 | 6.92 | 17.99 | 4.95 |
| $\delta^{13}C_{POC}$ (‰) | Max | −24.72 | −22.28 | −26.04 | −25.98 | −28.53 | −27.17 |
| | Min | −30.10 | −31.91 | −31.04 | −30.78 | −33.89 | −35.30 |
| | Mean | −27.97 | −28.79 | −29.27 | −28.26 | −30.96 | −29.97 |
| | SD | 2.38 | 4.40 | 2.25 | 1.26 | 1.49 | 2.03 |
| | CV (%) | 8.51 | 15.28 | 7.69 | 4.46 | 4.81 | 6.77 |

-: not measured; SD: standard deviation; CV: coefficient of variance, a statistic that measures the variability of each value when the mean value or the unit is not the same. CV = (SD / Mean) × 100%.

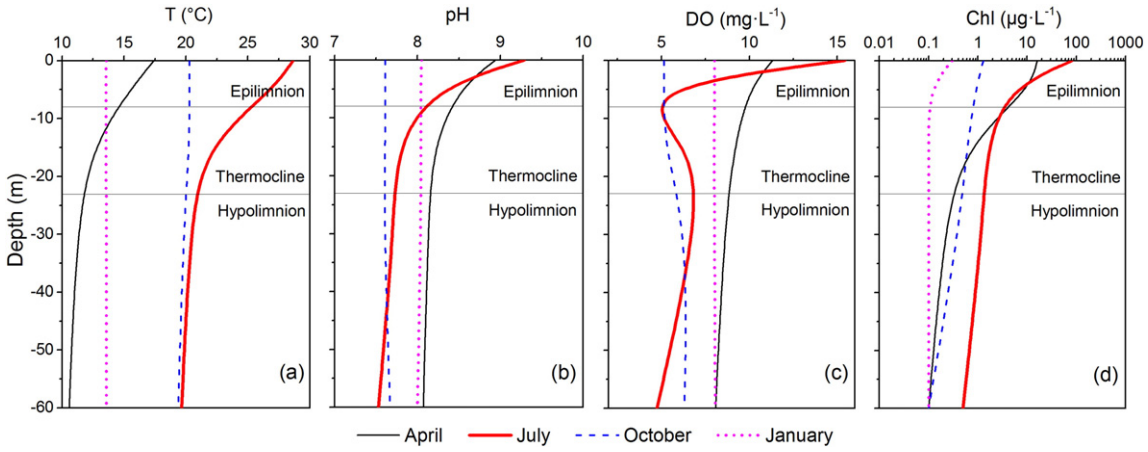


**Fig. 2.** Water profiles for T (a), pH (b), DO (c) and chlorophyll (d) in different seasons in the reservoir (W2).

between 2007–2008 and 2011–2012, but both surveys showed that DIC concentration varied similarly between sites (Fig. 3c, d). Average $\delta^{13}C_{DIC}$ was −8.48‰ in the inflow water, −7.54‰ in the reservoir, and −8.96‰ in the released water. $\delta^{13}C_{DIC}$ in the inflow and released waters varied synchronously and slightly, but $\delta^{13}C_{DIC}$ in the reservoir fluctuated greatly. In the reservoir, $\delta^{13}C_{DIC}$ was higher in the warm seasons than in the cold seasons, with a maximum of −4.92‰ (Fig. 3e, f). Overall, the released water had the highest DIC concentration and most negative $\delta^{13}C_{DIC}$.

In contrast to $\delta^{13}C_{DIC}$, DIC concentration showed seasonal variation in the water column (Fig. 4b, d). DIC concentration was highest in the surface water with values of 2479.22 μmol/L in autumn and 2247.34 μmol/L in summer when it was the lowest. $\delta^{13}C_{DIC}$ was most negative in autumn, with a value of −9.99‰, and most positive in spring, with a value of −6.78‰. DIC concentration and $\delta^{13}C_{DIC}$ became stratified in spring. In summer, when the stratification structure was most stable and water depth increased, the DIC concentration increased by 435.25 μmol/L, and $\delta^{13}C_{DIC}$ decreased by 2.00‰. In autumn and winter, with the collapse of thermal stratification, DIC concentration and $\delta^{13}C_{DIC}$ fluctuated slightly. The averages of $\delta^{13}C_{DIC}$ were −8.07‰ in April, −8.80‰ in July, −9.80‰ in October, and −8.99‰ in January.

### 3.4. POC

Average POC concentrations were 26.04 μmol/L in the inflow water, 62.32 μmol/L in the reservoir, and 24.25 μmol/L in the released water. The concentrations varied slightly in the inflow and released waters and greatly in the reservoir, where the concentration was higher in the warm seasons than in the cold seasons (Fig. 3g). Average $\delta^{13}C_{POC}$ was −28.11‰ in the inflow water, −29.88‰ in the reservoir, and −29.62‰ in the released water. There was no seasonal variation in $\delta^{13}C_{POC}$ in the river and released water, but $\delta^{13}C_{POC}$ in the reservoir was more negative in the warm seasons than in the cold seasons (Fig. 3h).

In the water profile, the $\delta^{13}C_{POC}$ of the surface water was most positive in summer, with a value of −22.28‰, and most negative in autumn, with a value of −31.91‰. In summer, there was a distinct gradient in $\delta^{13}C_{POC}$, which decreased by 4.55‰ from the surface to the bottom. The stratification did not completely disappear in autumn, and $\delta^{13}C_{POC}$ fluctuated greatly at the edge of the hypolimnion. In winter, $\delta^{13}C_{POC}$ was homogenized (Fig. 4e).

### 3.5. DOC

Average DOC concentrations were 128.24 μmol/L in the inflow water, 207.99 μmol/L in the reservoir, and 138.09 μmol/L in the released water. These concentrations are comparable to those from the Hongfeng and Baihua reservoirs (Li et al., 2008a, b) but higher than the concentration of Lake Baikal (Yoshioka et al., 2002). The amplitude of the variation in DOC concentration in the reservoir was larger than the amplitudes in the inflow and released waters, and there were two peaks in April and July (Fig. 3i). DOC concentration usually decreased with depth, and the average concentration was higher in the epilimnion (248.99 μmol/L) than in the hypolimnion (148.18 μmol/L; Fig. 4c).

## 4. Theoretical background: C biogeochemical cycle in a canyon reservoir

Carbon pools mainly include DOC, DIC (referring to the carbonate system: $CO_3^{2-}$, $HCO_3^-$, and $CO_2$), POC, and particulate inorganic C (PIC). Riverine DIC mainly comes from the chemical weathering of rocks. POC and DOC are primarily derived from soil erosion in drainage basins. The oxidation of organic matter produces a large amount of $CO_2$, and the partial pressure of $CO_2$ is considerably higher in rivers than in the atmosphere, making rivers a $CO_2$ source (Wang et al., 2007). Fig. 5 illustrates the C biogeochemical cycle in a canyon reservoir. The reservoir shows a tendency of limnological development. Phytoplankton consumes DIC and generates POC via photosynthesis. Some of the produced POC enters the aquatic food web through zooplankton, and other particles settle down due to gravity. During sedimentation, some POC is transformed into DIC by microbial respiration, while a portion deposits at the bottom of the reservoir. Autochthonous organic C can be mineralised to inorganic C under both aerobic and anaerobic conditions, but allochthonous organic C can only be mineralised under aerobic conditions (Hulthe et al., 1998; Bastviken et al., 2004). Some DOC is rapidly photodegraded to DIC in the epilimnion. Most DOC is consumed by microbes in the process of sedimentation, and only a small portion accumulates for a long time before being decomposed (Stedmon and Markager, 2005). The resuspension and degradation of sediment organic matter (SOM) can contribute to the formation of organic C. POC can also generate DOC by microbial decomposition. Additionally, SOM can generate $CH_4$ under the action of microbes. In the process of upward migration, the majority of the $CH_4$ is oxidized to $CO_2$ (Rinta et al., 2015). Riverine PIC is primarily derived from the erosion of basin rocks and $CaCO_3$ crystals with $CO_2$ degassing (authigene PIC) (Meybeck, 1993; Hellings et al., 1999). The consumption of $CO_2$ by photosynthesis in the reservoir can also lead to $CaCO_3$ crystals, which are biogenic PIC. The released water inherits the C biogeochemical characteristics of the bottom water in the reservoir.

## 5. Discussion

### 5.1. Factors controlling the carbon cycle in the Wujiang river-reservoir system

The C cycle in the karst river system demonstrates noticeable spatial heterogeneity caused by dam interception. The fundamental reasons for

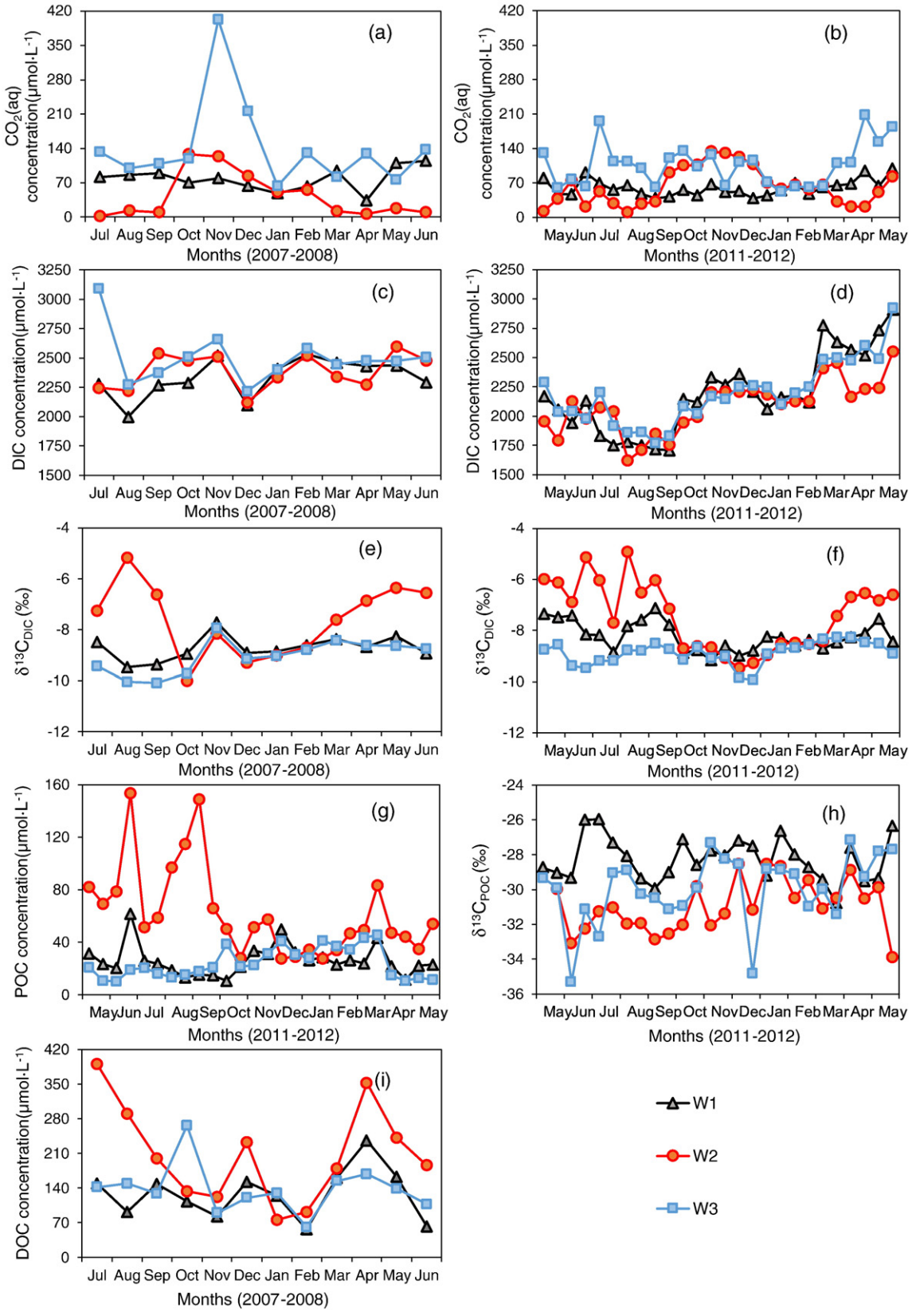


**Fig. 3.** Temporal variation in C concentrations and $\delta^{13}C$ in the river, reservoir and released water. (a) $CO_2$(aq), 2007–2008; (b) $CO_2$(aq), 2011–2012; (c) DIC, 2007–2008; (d) DIC, 2011–2012; (e) $\delta^{13}C_{DIC}$, 2007–2008; (f) $\delta^{13}C_{DIC}$, 2011–2012; (g) POC, 2011–2012; (h) $\delta^{13}C_{POC}$, 2011–2012; (i) DOC, 2007–2008.

this phenomenon are thermal stratification, enhanced biological activity, and the discharge of bottom water in the reservoir. In summer, the T of the surface water in the reservoir continuously increases due to solar radiation, and the warmer water T hinders the vertical mixing of the waters. Therefore, the water body forms a seasonal thermal stratification. With an increase in water depth, light intensity decreases and

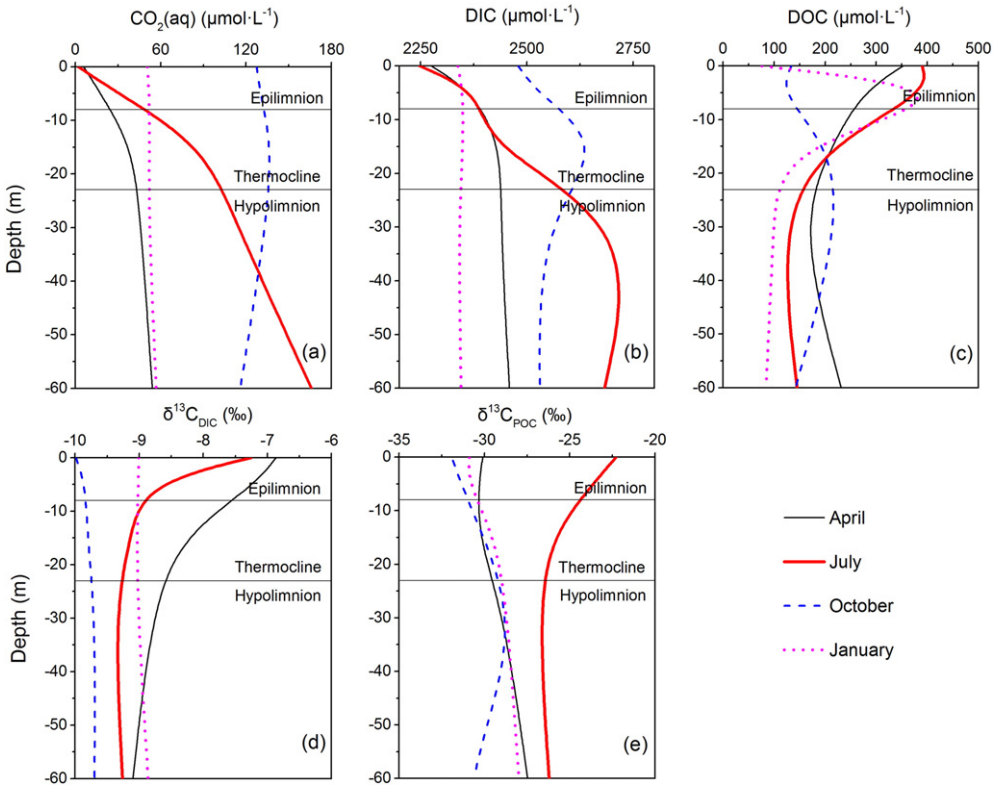


**Fig. 4.** Water profiles for C concentrations and $\delta^{13}C$ in different seasons in the reservoir (W2). (a) $CO_2$(aq); (b) DIC; (c) DOC; (d) $\delta^{13}C_{DIC}$; (e) $\delta^{13}C_{POC}$.

biological stratification gradually appears (Wetzel, 2001; Boehrer and Schultze, 2008). Furthermore, under biological action and thermodynamic equilibrium, C concentrations and isotope composition in the water profile gradually form a chemical stratification from April to September (Fig. 4). The reservoir surface water showed a higher POC concentration and a lower $CO_2$(aq) concentration due to strengthened photosynthesis, and the reservoir bottom water showed a higher $CO_2$(aq) concentration due to the intense microbial mineralisation of organic C. Meanwhile, the released water containing the bottom water in the reservoir had a higher $CO_2$ concentration. Based on the correlation analysis (Table 3), one can see that in the reservoir, an increase in T stimulated phytoplankton growth, and the phytoplankton assimilated more DIC. Biomass production accordingly increased, which was accompanied by an increase in pH and DO. However, for the river and released water, these correlations did not exist (Table 3). These findings suggested that the C cycle in the reservoir was mainly driven by biological activity (Fig. 5).

Reservoir DOC was influenced by allochthonous terrestrial input and autochthonous biological processes, which is consistent with the findings for DOC in natural lakes (Sugiyama et al., 2004). The high DOC concentrations in April (the rainy season) and July may have derived from terrestrial organic matter and the release of phytoplankton, respectively. In the water profile, some DOC is rapidly photodegraded in the euphotic zone, and the rest is mineralised at depth (Sugiyama et al., 2004; Kim et al., 2006). However, relatively high DOC concentrations at shallow water depths were sometimes found, which might have been due to the degradation of POC (Tranvik et al., 2009). The temporal fluctuations of C pools ($CO_2$, DIC, DOC, and POC) and their related

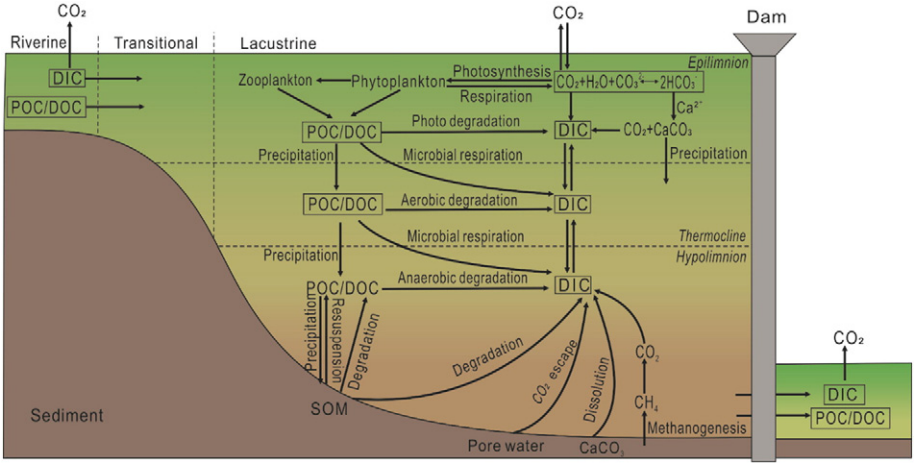


**Fig. 5.** Sketch map for the carbon biogeochemical cycle in a canyon reservoir. Degradation – due to microbes or other conditions, the transformation of organic matter into inorganic matter. Microbial respiration - under aerobic or anaerobic conditions, the process of microbial decomposition of organic matter. This process will continue during precipitation of organic matter. Methanogenesis - the process of generating $CH_4$ via the decomposition of SOM by microbes.

**Table 3**
Results of Pearson's correlation coefficient analysis between chlorophyll and other variables in different sampling sites.

| Sites | T | pH | DO | $CO_2$(aq) | DIC | POC | $\delta^{13}C_{DIC}$ | $\delta^{13}C_{POC}$ |
|---|---|---|---|---|---|---|---|---|
| W1 | 0.061 | −0.008 | 0.15 | −0.058 | −0.012 | 0.367 | 0.32 | −0.44* |
| W2 | 0.515** | 0.701** | 0.505** | −0.57** | −0.335** | 0.929** | 0.642** | 0.105 |
| W3 | −0.269 | 0.281 | 0.349* | −0.266 | −0.098 | 0.495* | 0.347* | −0.19 |

** Correlation is significant at the 0.01 level (2-tailed).
* Correlation is significant at the 0.05 level (2-tailed).

isotopic compositions ($\delta^{13}C_{DIC}$ and $\delta^{13}C_{POC}$) in the reservoir and released water were far greater than those in the inflow water, and the coefficients of variance for different variables in the reservoir were generally larger (Table 2). These results suggest that dam interception dramatically enhances the C biogeochemical cycle, especially in warm seasons.

### 5.2. Carbon isotope tracing in the Wujiang river-reservoir system

The $\delta^{13}C$ of soil $CO_2$ in the Wujiang basin was shown to be approximately −23‰ (Li et al., 2008a, b), and the dissolution of soil $CO_2$ in soil water leads to an average $\delta^{13}C$ of −17‰ (Telmer and Veizer, 1999). As a result, chemical weathering of marine carbonates ($\delta^{13}C \approx 0$‰) by this soil water (Andrews et al., 2001) generally produces DIC with a $\delta^{13}C$ of about −8.5‰. The $\delta^{13}C_{DIC}$ in the river varied slightly, with an average of −8.48‰, suggesting that chemical weathering of carbonates mainly affects the DIC in the river. Likewise, from November to February, the $\delta^{13}C_{DIC}$ values of all samples in the reservoir and released water were about −8.5‰ (Fig. 3e, f), indicating limits on carbonate weathering in the cold seasons. $\delta^{13}C_{DIC}$ is mainly affected by two mechanisms. First, $CO_2$ exchange at the water-gas interface can affect $\delta^{13}C_{DIC}$. The dissolving process of atmospheric $CO_2$ has a fractionation of −1.29‰ to −1.19‰ (Zhang et al., 1995), and $CO_2$ outgassing may lead to $^{13}C$ enrichment in DIC (Doctor et al., 2008). Some samples in the river were above and below the dissolution line of carbonate (Fig. 6a), indicating the influence of $CO_2$ outgassing and respired $CO_2$, respectively (van Breugel et al., 2005; Doctor et al., 2008). Second, Photosynthesis and respiration can also affect $\delta^{13}C_{DIC}$. Phytoplankton preferentially absorb light C isotopes ($^{12}C$), leading to $^{13}C$ enrichment of residual inorganic C. The process of DIC production in respiration has no large isotope fractionation, but the decomposition of organic C preferentially releases $^{12}C$ (van Breugel et al., 2005), resulting in more negative $\delta^{13}C_{DIC}$ in the bottom waters. This finding is clearly confirmed by the variation in $\delta^{13}C_{DIC}$ in the vertical profiles (Fig. 4d). This pattern is consistent with several meromictic lakes (Deevey et al., 1963; Rau, 1978) but inconsistent with some small European lakes, where higher $\delta^{13}C_{DIC}$ in the bottom was attributed to the dissolution of authigenic $CaCO_3$ or acetotrophic methanogenesis (Rinta et al., 2015). In spring and summer, due to the different intensity of biological activity, $\delta^{13}C_{DIC}$ did not decrease to the same degree. Photosynthesis and respiration were the major factors controlling $\delta^{13}C_{DIC}$ in the reservoir, and $\delta^{13}C_{DIC}$ was therefore significantly correlated with $CO_2$ ($n = 86$, $r = -0.673$, $p < 0.001$. Fig. 6a).

There are three major sources of POC in the water: (i) Terrestrial plants from the basin. The average $\delta^{13}C$ of terrestrial C3 plants (3C compound as the initial product in photosynthesis) and C4 plants (4C compound as the initial product in photosynthesis) are −27‰ and −12‰, respectively (Vogel, 1993). Riverine POC is mainly from terrestrial C3 plant debris, and the average $\delta^{13}C_{POC}$ remained around −28‰ (Fig. 3h). (ii) Aquatic phytoplankton. The $\delta^{13}C$ of freshwater phytoplankton ranges from −34.4‰ to −5.9‰ (Vuorio et al., 2006; Brutemark et al., 2009). (iii) Microbial biomass. Microbes provide $^{13}C$-depleted biomass. Chemoautotrophic and methanotrophic microbes can provide biomass with a $\delta^{13}C$ of about −45‰ and −65‰ to −50‰, respectively (Whiticar et al., 1986; Freeman et al., 1990). In summer, the POC in the surface water was extremely enriched in $^{13}C$ (Fig. 4e) mainly because $HCO_3^-$ was an inorganic C source under $CO_2$ limitation during intense photosynthesis, which weakens the discrimination of $^{13}C$ and enriches organic compounds with $^{13}C$ (Fogel and Cifuentes, 1993). In addition to photoautotrophic biomass settling from the epilimnion, the POC in the hypolimnion also included $^{13}C$-depleted microbial biomass due to intense biological activity. A study in eutrophic Lake Mendota (USA) is consistent with this finding (Hollander and Smith, 2001). The above reasoning explains why the vertical variation in $\delta^{13}C_{POC}$ in summer was distinct from other seasons (Fig. 4e). In other seasons, phytoplankton assimilates the isotopically light $CO_2$ as a C source, resulting in $^{13}C$ depletion in the surface water POC. With an increase in water depth, a large amount of organic matter is decomposed, and this process preferentially releases $^{12}C$ and leaves the residual organic C enriched in $^{13}C$ (van Breugel et al., 2005; Vähätalo and Wetzel, 2008). Due to low biological activity associated with low water T in spring and winter, the vertical $\delta^{13}C_{POC}$ varied slightly. In autumn, an abrupt shift of $\delta^{13}C_{POC}$ in the hypolimnion (Fig. 4e) may be attributed to the contribution of isotopically depleted algae.

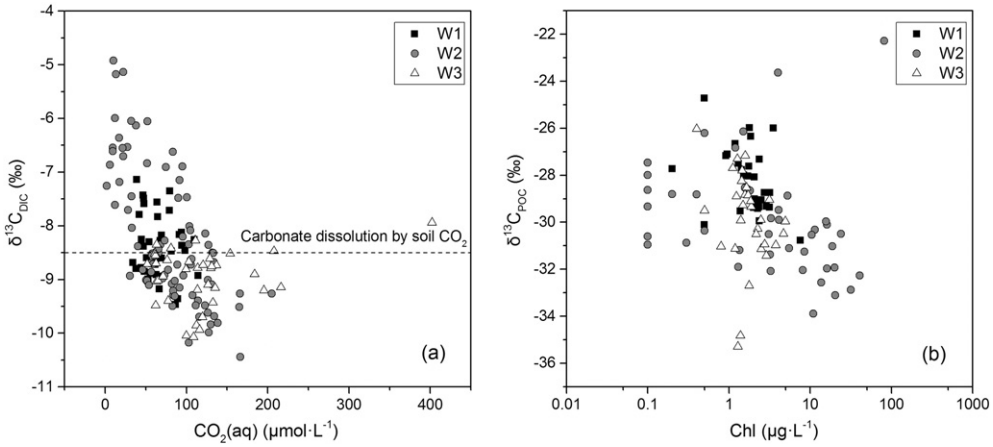


**Fig. 6.** Scatter plots of $CO_2$(aq) versus $\delta^{13}C_{DIC}$ (a) and Chl versus $\delta^{13}C_{POC}$ (b) in the Wujiang river-reservoir system.

These observations provide strong field evidence that $\delta^{13}C_{DIC}$ and $\delta^{13}C_{POC}$ are significantly influenced by biologically mediated processes. Therefore, these metrics can be used to trace the C biogeochemical cycle in the karst river-reservoir system.

## 6. Conclusions

The C species and related $\delta^{13}C$ showed remarkable heterogeneity in time and space in the Wujiang karst river-reservoir system. Thermal and chemical stratifications had significant influences on the water released from the reservoir. Evidence from $\delta^{13}C$ demonstrated that the C system was primarily influenced by carbonate weathering in the karst river and by algal activity in the reservoir. Compared to the water in the river, the reservoir and released water showed higher coefficients of variance for different C species, suggesting that after damming, biological activity became a key controlling factor and accelerated the C biogeochemical cycle. The results of this study have important implications for understanding the C cycle in elongated and deep reservoirs. Moreover, the temporal variation in C species suggests high-frequency measurements would produce a more accurate and reliable estimation of the C budget in impounded rivers.

## Acknowledgements

This study was financially supported by the National Key R & D Programme of China (2016YFA0601001), the National Natural Science Foundation of China (Grant Nos. U1612441 and 41473082), and the CAS "Light of West China" Program.

## References

Andrews, J.E., Greenaway, A.M., Dennis, P.F., Barnes-Leslie, D.A., 2001. Isotopic effects on inorganic carbon in a tropical river caused by caustic discharges from bauxite processing. Appl. Geochem. 16:197–206. https://doi.org/10.1016/S0883-2927(00)00033-0.

Atekwana, E.A., Krishnamurthy, R.V., 1998. Seasonal variations of dissolved inorganic carbon and $\delta^{13}C$ of surface water: application of a modified gas evolution technique. J. Hydrol. 205:265–278. https://doi.org/10.1016/S0022-1694(98)00080-8.

Aufdenkampe, A.K., Mayorga, E., Raymond, P.A., Melack, J.M., Doney, S.C., Alin, S.R., Aalto, R.E., Yoo, K., 2011. Riverine coupling of biogeochemical cycles between land, oceans, and atmosphere. Front. Ecol. Environ. 9:53–60. https://doi.org/10.1890/100014.

Barros, N., Cole, J.J., Tranvik, L.J., Prairie, Y.T., Bastviken, D., Huszar, V.L.M., Giorgio, P.D., Roland, F., 2011. Carbon emission from hydroelectric reservoirs linked to reservoir age and latitude. Nat. Geosci. 4:593–596. https://doi.org/10.1038/ngeo1211.

Bastviken, D., Persson, L., Odham, G., Tranvik, L.J., 2004. Degradation of dissolved organic matter in oxic and anoxic lake water. Limnol. Oceanogr. 49:109–116. https://doi.org/10.4319/lo.2004.49.1.0109.

Boehrer, B., Schultze, M., 2008. Stratification of lakes. Rev. Geophys. 46:620–628. https://doi.org/10.1029/2006RG000210.

Brutemark, A., Lindehoff, E., Granéli, E., Granéli, W., 2009. Carbon isotope signature variability among cultured microalgae: influence of species, nutrients and growth. J. Exp. Mar. Biol. Ecol. 372:98–105. https://doi.org/10.1016/j.jembe.2009.02.013.

Buchanan, D.L., Corcoran, B.J., 1959. Sealed tube combustions for determination of carbon-14 and total carbon. Anal. Chem. 31:1635–1638. https://doi.org/10.1021/ac60154a025.

Chetelat, B., Liu, C.Q., Zhao, Z.Q., Wang, Q., Li, S.L., Li, J., Wang, B., 2008. Geochemistry of the dissolved load of the Changjiang Basin rivers: anthropogenic impacts and chemical weathering. Geochim. Cosmochim. Acta 72:4254–4277. https://doi.org/10.1016/j.gca.2008.06.013.

Cole, J.J., Prairie, Y.T., Caraco, N.F., Mcdowell, W.H., Tranvik, L.J., Striegl, R.G., Duarte, C.M., Kortelainen, P., Downing, J.A., Middelburg, J.J., Melack, J., 2007. Plumbing the global carbon cycle: integrating inland waters into the terrestrial carbon budget. Ecosystems 10:171–184. https://doi.org/10.1007/s10021-006-9013-8.

Deevey, E.S., Nakai, N., Stuiver, M., 1963. Fractionation of sulfur and carbon isotopes in a meromictic lake. Science 139:407–408. https://doi.org/10.1126/science.139.3553.407 (Source: PubMed).

Doctor, D.H., Kendall, C., Sebestyen, S.D., Shanley, J.B., Ohte, N., Boyer, E.W., 2008. Carbon isotope fractionation of dissolved inorganic carbon (DIC) due to outgassing of carbon dioxide from a headwater stream. Hydrol. Process. 22:2410–2423. https://doi.org/10.1002/hyp.6833.

Fogel, M.L., Cifuentes, L.A., 1993. Isotope Fractionation During Primary Production. Springer, US, pp. 73–98.

Freeman, K.H., Hayes, J.M., Trendel, J.M., Albrecht, P., 1990. Evidence from carbon isotope measurements for diverse origins of sedimentary hydrocarbons. Nature 343:254–256. https://doi.org/10.1038/343254a0 (Source: PubMed).

Hellings, L., Dehairs, F., Tackx, M., Keppens, E., Baeyens, W., 1999. Origin and fate of organic carbon in the freshwater part of the Scheldt Estuary as traced by stable carbon isotope composition. Biogeochemistry 47:167–186. https://doi.org/10.1007/BF00994921.

Hollander, D.J., Smith, M.A., 2001. Microbially mediated carbon cycling as a control on the $\delta^{13}C$ of sedimentary carbon in eutrophic Lake Mendota (USA): new models for interpreting isotopic excursions in the sedimentary record. Geochim. Cosmochim. Acta 65:4321–4337. https://doi.org/10.1016/S0016-7037(00)00506-8.

Hulthe, G., Hulth, S., Hall, P.O.J., 1998. Effect of oxygen on degradation rate of refractory and labile organic matter in continental margin sediments. Geochim. Cosmochim. Acta 62:1319–1328. https://doi.org/10.1016/S0016-7037(98)00044-1.

Humborg, C., Conley, D.J., Rahm, L., Wulff, F., Cociasu, A., Ittekkot, V., 2000. Silicon retention in river basins: far-reaching effects on biogeochemistry and aquatic food webs in coastal marine environments. Ambio 29:45–50. https://doi.org/10.1639/0044-7447(2000)029[0045: SRIRBF]2.0.CO;2.

Karr, J.R., 1991. Biological integrity: a long-neglected aspect of water resource management. Ecol. Appl. 1:66–84. https://doi.org/10.2307/1941848.

Khadka, M.B., Martin, J.B., Jin, J., 2014. Transport of dissolved carbon and $CO_2$ degassing from a river system in a mixed silicate and carbonate catchment. J. Hydrol. 513:391–402. https://doi.org/10.1016/j.jhydrol.2014.03.070.

Kim, C., Nishimura, Y., Nagata, T., 2006. Role of dissolved organic matter in hypolimnetic mineralization of carbon and nitrogen in a large, monomictic lake. Limnol. Oceanogr. 51:70–78. https://doi.org/10.4319/lo.2006.51.1.0070.

Kummu, M., Varis, O., 2007. Sediment-related impacts due to upstream reservoir trapping, the Lower Mekong River. Geomorphology 85:275–293. https://doi.org/10.1016/j.geomorph.2006.03.024.

Li, S.L., Liu, C.Q., Lang, Y., Tao, F., Zhao, Z.Q., 2008a. Stable carbon isotope biogeochemistry and anthropogenic impacts on karst ground water, Zunyi, Southwest China. Aquat. Geochem. 14:211–221. https://doi.org/10.1007/s10498-008-9033-4.

Li, W., Wu, F.C., Liu, C.Q., Fu, P.Q., Wang, J., Mei, Y., Wang, L., Guo, J.Y., 2008b. Temporal and spatial distributions of dissolved organic carbon and nitrogen in two small lakes on the Southwestern China Plateau. Limnology 9:163–171. https://doi.org/10.1007/s10201-008-0241-9.

Liu, Z., Dreybrodt, W., 2015. Significance of the carbon sink produced by $H_2O$-carbonate-$CO_2$-aquatic phototroph interaction on land. Sci. Bull. 60:182–191. https://doi.org/10.1007/s11434-014-0682-y.

Liu, C.Q., Wang, F., Wang, Y., Wang, B., 2009. Responses of aquatic environment to river damming-from the geochemical view. Resour. Environ. Yangtze Basin 18, 384–396.

Maberly, S.C., 1996. Diel, episodic and seasonal changes in pH and concentrations of inorganic carbon in a productive lake. Freshw. Biol. 35:579–598. https://doi.org/10.1111/j.1365-2427. 1996.tb01770.x.

Mccartney, M.P., Sullivan, C.A., Acreman, M.C., 2001. Ecosystem Impacts of Large Dams. Centre for Ecology & Hydrology.

Meybeck, M., 1993. Riverine transport of atmospheric carbon: sources, global typology and budget. Water Air Soil Pollut. 70:443–463. https://doi.org/10.1007/BF01105015.

Peng, X., Liu, C.Q., Wang, B., Zhao, Y.C., 2014. The impact of damming on geochemical behavior of dissolved inorganic carbon in a karst river. Sci. Bull. 59:2348–2355. https://doi.org/10.1007/s11434-014-0153-5.

Rau, G.H., 1978. Carbon-13 depletion in a subalpine lake: carbon flow implications. Science 201, 901–902.

Regnier, P., Friedlingstein, P., Ciais, P., Mackenzie, F.T., Gruber, N., Janssens, I.A., Laruelle, G.G., Lauerwald, R., Luyssaert, S., Andersson, A.J., 2013. Anthropogenic perturbation of the carbon fluxes from land to ocean. Nat. Geosci. 6:597–607. https://doi.org/10.1038/ngeo1830.

Rinta, P., Bastviken, D., van Hardenbroek, M., Kankaala, P., Leuenberger, M., Schilder, J., Stötter, T., Heiri, O., 2015. An inter-regional assessment of concentrations and $\delta^{13}C$ values of methane and dissolved inorganic carbon in small European lakes. Aquat. Sci. 77:667–680. https://doi.org/10.1007/s00027-015-0410-y.

Sironić, A., Barešić, J., Horvatinčić, N., Brozinčević, A., Vurnek, M., Kapelj, S., 2016. Changes in the geochemical parameters of karst lakes over the past three decades-the case of Plitvice Lakes, Croatia. Appl. Geochem. 78:12–22. https://doi.org/10.1016/j.apgeochem.2016.11.013.

Stedmon, C.A., Markager, S., 2005. Tracing the production and degradation of autochthonous fractions of dissolved organic matter by fluorescence analysis. Limnol. Oceanogr. 50:1415–1426. https://doi.org/10.2307/3597686.

Sugiyama, Y., Anegawa, A., Kumagai, T., Harita, Y., Hori, T., Sugiyama, M., 2004. Distribution of dissolved organic carbon in lakes of different tropic types. Limnology 5:165–176. https://doi.org/10.1007/s10201-004-0128-3.

Telmer, K., Veizer, J., 1999. Carbon fluxes, $pCO_2$ and substrate weathering in a large northern river basin, Canada: carbon isotope perspectives. Chem. Geol. 159:61–86. https://doi.org/10.1016/S0009-2541(99)00034-0.

Tranvik, L.J., Downing, J.A., Cotner, J.B., Loiselle, S.A., Striegl, R.G., Ballatore, T.J., Dillon, P., Finlay, K., Fortino, K., Knoll, L.B., Kortelainen, P.L., Kutser, T., Larsen, S., Laurion, I., Leech, D.M., McCallister, S.L., McKnight, D.M., Melack, J.M., Overholt, E., Porter, J.A., Prairie, Y., Renwick, W.H., Roland, F., Sherman, B.S., Schindler, D.W., Sobek, S., Tremblay, A., Vanni, M.J., Verschoor, A.M., Wachenfeldt, E.V., Weyhenmeyer, G.A., 2009. Lakes and reservoirs as regulators of carbon cycling and climate. Limnol. Oceanogr. 54:2298–2314. https://doi.org/10.4319/lo.2009.54.6_part_2.2298.

van Breugel, Y., Schouten, S., Paetzel, M., Nordeide, R., Damsté, J.S.S., 2005. The impact of recycling of organic carbon on the stable carbon isotopic composition of dissolved inorganic carbon in a stratified marine system (Kyllaren fjord, Norway). Org. Geochem. 36:1163–1173. https://doi.org/10.1016/S0140-6701(06)81058-1.

Vähätalo, A.V., Wetzel, R.G., 2008. Long-term photochemical and microbial decomposition of wetland-derived dissolved organic matter with alteration of $^{13}C$:$^{12}C$ mass ratio. Limnol. Oceanogr. 53:1387–1392. https://doi.org/10.2307/40058260.

Vogel, J.C., 1993. Variability of carbon isotope fractionation during photosynthesis. Stable Isot. Plant Carbon-Water Relat. 7, pp. 29–46.

Vuorio, K., Meili, M., Sarvala, J., 2006. Taxon-specific variation in the stable isotope signatures ($\delta^{13}C$ and $\delta^{15}N$) of lake phytoplankton. Freshw. Biol. 51:807–822. https://doi.org/10.1111/j.1365-2427.2006.01529.x.

Wang, S.J., Li, R.L., Sun, C.X., Zhang, D.F., Li, F.Q., Zhou, D.Q., Xiong, K.N., Zhou, Z.F., 2004. How types of carbonate rock assemblages constrain the distribution of karst rocky desertified land in Guizhou Province, PR China: phenomena and mechanisms. Land Degrad. Dev. 15:123–131. https://doi.org/10.1002/ldr.591.

Wang, F., Wang, Y., Zhang, J., Xu, H., Wei, X., 2007. Human impact on the historical change of $CO_2$ degassing flux in River Changjiang. Geochem. Trans. 8, 7.

Wang, F., Yu, Y., Liu, C.Q., Wang, B., Wang, Y., Guan, J., Mei, H.Y., 2010. Dissolved silicate retention and transport in cascade reservoirs in Karst area, Southwest China. Sci. Total Environ. 408:1667–1675. https://doi.org/10.1016/j.scitotenv.2010.01.017 (Source: PubMed).

Wang, B., Liu, C.Q., Peng, X., Wang, F., 2013. Mechanisms controlling the carbon stable isotope composition of phytoplankton in karst reservoirs. J. Limnol. 72:127–139. https://doi.org/10.4081/jlimnol. 2013.e11.

Wang, F., Cao, M., Wang, B., Ma, J., 2015. Seasonal variation of $CO_2$ diffusion flux from a large subtropical reservoir in East China. Atmos. Environ. 103:129–137. https://doi.org/10.1016/j.atmosenv.2014.12.042.

Wetzel, R.G., 2001. Limnology: lake and river ecosystems. EOS Trans. Am. Geophys. Union 21:1–9. https://doi.org/10.1016/B978-0-08-057439-4.50017-4.

Whiticar, M.J., Faber, E., Schoell, M., 1986. Biogenic methane formation in marine and freshwater environments: $CO_2$ reduction *vs.* acetate fermentation-isotope evidence. Geochim. Cosmochim. Acta 50:693–710. https://doi.org/10.1016/0016-7037(86)90346-7.

Yoshioka, T., Ueda, S., Khodzher, T., Bashenkhaeva, N., Korovyakova, I., Sorokovikova, L., Gorbunova, L., 2002. Distribution of dissolved organic carbon in Lake Baikal and its watershed. Limnology 3:159–168. https://doi.org/10.1007/s102010200019.

Zeng, C., Liu, Z., Zhao, M., Yang, R., 2016. Hydrologically-driven variations in the karst-related carbon sink fluxes: insights from high-resolution monitoring of three karst catchments in Southwest China. J. Hydrol. 533:74–90. https://doi.org/10.1016/j.jhydrol.2015.11.049.

Zhang, J., Quay, P.D., Wilbur, D.O., 1995. Carbon isotope fractionation during gas-water exchange and dissolution of $CO_2$. Geochim. Cosmochim. Acta 59:107–114. https://doi.org/10.1016/00167-0379(59)1550D-.

Zhou, J., Zhang, M., Lu, P., 2013. The effect of dams on phosphorus in the middle and lower Yangtze river. Water Resour. Res. 49:3659–3669. https://doi.org/10.1002/wrcr.20283.